

# Cavitation in a swollen elastomer constrained by a non-swellable shell

Huiming Wang<sup>1,2</sup> and Shengqiang Cai<sup>3,a)</sup>

<sup>1</sup>Department of Engineering Mechanics, Zhejiang University, Hangzhou 310027, People's Republic of China

<sup>2</sup>Soft Matter Research Center (SMRC), Zhejiang University, Hangzhou 310027, People's Republic of China

<sup>3</sup>Department of Mechanical and Aerospace Engineering, University of California, San Diego, La Jolla, California 92093, USA

(Received 14 January 2015; accepted 3 April 2015; published online 15 April 2015)

A small cavity inside a swollen elastomer may grow or shrink, depending on the external stresses applied onto the elastomer, surrounding humidity, and boundary constraints of the elastomer. In this article, we study the variation of the size of a small cavity inside a swollen elastomer when environmental humidity changes. In the model, the surface of the swollen elastomer is coated by a non-swellable but permeable elastomer shell. Our analysis shows that the cavity shrinks with the increase of humidity, while the cavity grows with the decrease of humidity. Interestingly, with the decrease of the humidity, the cavity grows slowly and continuously first; when the humidity is lower than a critical value, the cavity may grow discontinuously, jumping from a small one to a big one, which is analogous to first-order phase transition. In this paper, we explore the effects of initial swelling ratio and the boundary constraint of the swollen elastomer on its cavitation behavior.

© 2015 AIP Publishing LLC. [<http://dx.doi.org/10.1063/1.4918278>]

## I. INTRODUCTION

Most elastomers can swell by imbibing solvent. The amount of solvent in the elastomer depends on the molecular interaction between solvent and the elastomer, external stresses applied onto the elastomer, and other external conditions such as humidity and temperature. In particular, some polymeric elastomers can absorb a large amount of water and swell significantly. Recently, swelling elastomers have been intensively explored in diverse applications, ranging from swellaible packers in oil field<sup>1</sup> to soft actuators and sensors.<sup>2–6</sup> In the applications of swollen elastomer, different mechanical instabilities have been observed and studied. For instance, it has been shown that creases, a newly identified mechanical instability mode, can form on the surface of a constrained swelling gel when its swelling ratio is beyond a critical value.<sup>7,8</sup> As another example, a hydrogel sheet with inhomogeneous distribution of swelling ratio can swell to various intriguing three-dimensional structures.<sup>9</sup> In this article, we study a new type of chemo-mechanical instabilities in a partially swollen elastomer: cavitation instability.

Cavitation in a dry elastomer has been recognized as one important failure mode.<sup>10–15</sup> An initially infinitesimal cavity inside an elastomer may grow continuously or discontinuously when the elastomer is subjected to internal or external stresses. Compared to cavitation instabilities in dry elastomers, cavity growth in a swollen elastomer has been much less studied. In particular, a swollen elastomer can respond to both mechanical and chemical stimuli, so the cavitation in a swollen elastomer depends on both mechanical and chemical loading conditions.

Cavitation or crack propagation in swollen elastomer, caused by osmosis, has been often observed in both engineering materials and biological materials. For example, osmosis-induced shrinkage of nucleus pulposus in degenerative intervertebral discs can cause propagation of cracks and expansion of cavities.<sup>16</sup> As another example, large cavities in some dried vegetables and fruits can be also frequently observed in daily life. In a recent paper, we have found that a small cavity in a fully swollen elastomer with constraint can grow discontinuously with decreasing the chemical potential of solvent in the environment.<sup>17</sup> In this paper, we extend our previous work and study cavitation instability in a partially swollen gel with elastic constraints. We further explore the influence of initial swelling ratio and the boundary constraint of the swollen elastomer on its cavitation behavior.

## II. MODEL OF CAVITATION

Fig. 1 sketches the model we are going to study in the article. A swollen elastomer containing a small cavity is coated by a non-swellable but permeable elastomer shell. The solvent in the elastomer is assumed to be water in our model. When the external humidity increases, the cavity in the swollen elastomer shrinks with the further swelling of the elastomer. When the humidity decreases, the cavity enlarges with deswelling of the elastomer core. To study the change of the cavity size with humidity, we will compute the total free energy of the whole system including the swollen elastomer core and the non-swellable elastomer shell as a function of the radius of the cavity.

As illustrated in Fig. 1, we take the initial state of a stress-free and partially swollen elastomer as reference state. The linear swelling ratio in the initial state is denoted by  $\lambda_0$ . Based on Flory-Rehner's theory,<sup>18,19</sup> Helmholtz free energy density of a swollen elastomer with deformation gradient  $F_{iK}$  is given by

<sup>a)</sup>Author to whom correspondence should be addressed. Electronic mail: shqcai@ucsd.edu

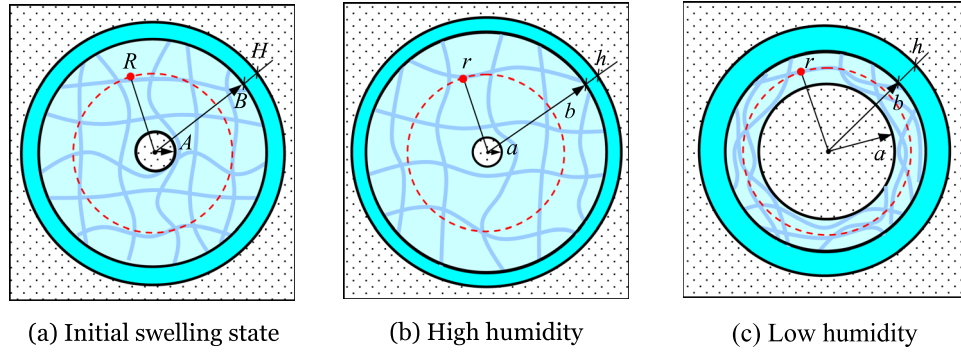


FIG. 1. A stress-free elastomer with initial swelling and a small cavity is taken as reference state. (a) The swollen elastomer is coated by a non-swelling but permeable elastomer shell. (b) At high humidity, the elastomer swells with decreasing the size of the cavity. (c) At low humidity, the swollen elastomer shrinks with enlarging the cavity size. A material point in the reference state marked by its radius  $R$  in (a) moves to  $r$  in the deformed state (b) and (c).

$$W_h = \frac{\lambda_0^{-3}}{2} NkT \left( \lambda_0^2 F_{iK} F_{iK} - 3 - 2 \log(\lambda_0^3 J) \right) - \frac{kT}{\Omega} \left[ \left( J - \lambda_0^3 \right) \log \left( \frac{J}{\lambda_0^3 J - 1} \right) + \frac{\chi}{\lambda_0^6 J} \right], \quad (1)$$

where  $N$  is the number of polymer chains per volume,  $k$  is the Boltzmann constant,  $T$  is the temperature,  $\Omega$  is the volume of a water molecule, and  $\chi$  is the dimensionless interaction parameter, which is set to be 0.2 in this study.  $N\Omega$  is a dimensionless measurement of elastic modulus of the polymer network, which is taken to be  $10^{-3}$  in our calculation.

Non-swelling elastomer is assumed to be incompressible neo-Hookean material, so the free energy density of the elastomer shell is

$$W_s = \frac{1}{2} G (F_{iK} F_{iK} - 3) - \Pi (\det(\mathbf{F}) - 1), \quad (2)$$

where  $G$  is small deformation shear modulus and  $\Pi$  is Lagrange multiplier.

A combination of the free energy density (1) and equilibrium thermodynamics gives the equation of state of a swollen elastomer,

$$\sigma_{ij} = \frac{NkT}{\lambda_0^3 J} \left( \lambda_0^2 F_{jK} F_{iK} - \delta_{ij} \right) + \frac{kT}{\Omega} \left[ \log \left( 1 - \frac{1}{\lambda_0^3 J} \right) + \frac{1}{\lambda_0^3 J} + \frac{\chi}{\lambda_0^6 J^2} - \frac{\mu}{kT} \right] \delta_{ij}, \quad (3)$$

where  $\sigma_{ij}$  is the true stress and  $\mu$  is the chemical potential of water in the environment, which can be determined by relative humidity ( $RH$ ) in the surrounding environment:  $\mu = kT \log(RH)$ .

Likewise, the equation of state for the non-swelling elastomer shell is

$$\sigma_{ij} = GF_{jK} F_{iK} - \delta_{ij} \Pi, \quad (4)$$

which is known as neo-Hookean model. The incompressibility condition of the elastomer shell can be written as  $\det(\mathbf{F}) = 1$ .

We assume the deformation in the core-shell structure illustrated in Fig. 1 is spherically symmetric, and a material

point in the reference state marked by  $R$  moves to  $r$  in the current state as shown in Fig. 1. Consequently, the hoop and radial stretches in the core-shell structure can be written as

$$\lambda_r = \frac{dr}{dR}, \quad (5)$$

$$\lambda_\theta = \frac{r}{R}, \quad (6)$$

in which  $r$  is a single variable function of  $R$ .

In a spherical coordinate system, force balance equation can be written as

$$\frac{d\sigma_r}{dr} + 2 \frac{\sigma_r - \sigma_\theta}{r} = 0. \quad (7)$$

Plugging Eqs. (3)–(6) into Eq. (7), we can obtain a second order ordinary differential equation of  $r(R)$  for both swollen elastomer core and the non-swelling elastomer shell.

Both radial stress and hoop stretch across the interface between the elastomer shell and the core are continuous, so we have

$$\sigma_r(R = B^+) = \sigma_r(R = B^-), \quad (8)$$

$$\lambda_\theta(R = B^+) = \lambda_\theta(R = B^-). \quad (9)$$

The outer surface of the elastomer shell is stress free, so,

$$\sigma_r(R = B + H) = 0. \quad (10)$$

In our model,  $A/B$  is set to be 1/50 and  $H/B = 0.256$ .

To investigate equilibrium configuration and possible instabilities of the core-shell system in different conditions, we compute the deformation field in the structure with different cavity size  $a$  (Fig. 1). Using the obtained deformation field, we calculate the Gibbs free energy of the core-shell system through the following integration:

$$F = \int_{V_1} (W_h - \mu C) dV + 4\pi a^2 \gamma + \int_{V_2} W_s dV, \quad (11)$$

where  $C$  is the concentration of water and  $\gamma$  is the surface energy density of the cavity, which is set to be  $\gamma \lambda_0 / NkTA = 20$ .  $V_1$  is the volume of the swollen elastomer and  $V_2$  is the volume of the non-swelling elastomer shell. In Eq. (11), we also take account of surface energy of the cavity.

**III. RESULTS AND DISCUSSIONS**

We first study the influences of initial swelling ratio of the elastomer core on the cavitation behaviors. Figures 2(a) and 2(b) plot the free energy landscape of the swollen elastomer constrained by a rigid shell with two different initial swelling ratios  $\lambda_0 = 1.436$  and  $\lambda_0 = 1.307$  for different environmental humidity. For certain ranges of humidity, free energy landscape in Figs. 2(a) and 2(b) shows double well structure, which is a reminiscent of first-order phase transition. When humidity is high, the swollen elastomer with a small cavity has the lowest free energy. When humidity is low, the swollen elastomer with a large cavity has the lowest energy. At a critical humidity, the swollen elastomer has two minimal free energy of the same magnitude, corresponding to a small cavity and a large cavity, respectively.

We assume that in equilibrium, the swollen elastomer stays in the configuration with lowest free energy as shown in Figs. 2(a) and 2(b). Figure 3 plots the cavity size in the elastomer as a function of humidity with two different initial swelling ratios. Discontinuous growth of cavity in the elastomer is illustrated in Fig. 3 for nonzero surface energy density. For comparison, Fig. 3 also plots the growth of cavity in the elastomer when surface energy is neglected. It can be seen from Fig. 3 that the growth of cavity in the elastomer

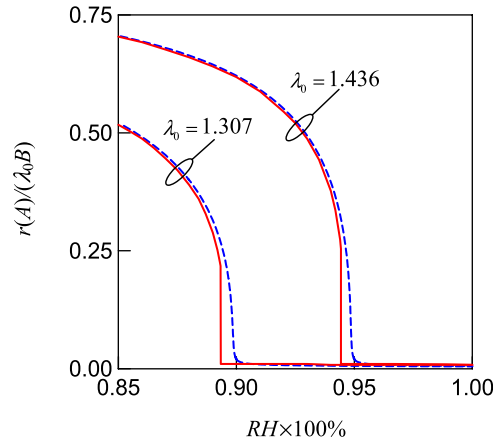


FIG. 3. The size of the cavity as a function of external humidity in a swollen elastomer constrained by a rigid shell. Solid line is for surface tension  $\gamma\lambda_0/(NkTA) = 20$  and the dashed line is for zero surface tension.

becomes continuous if surface tension of the cavity is negligible. The quantitative influences of initial swelling ratio of the elastomer on the cavitation behavior have also been shown in Fig. 3: discontinuous change of cavity size happens

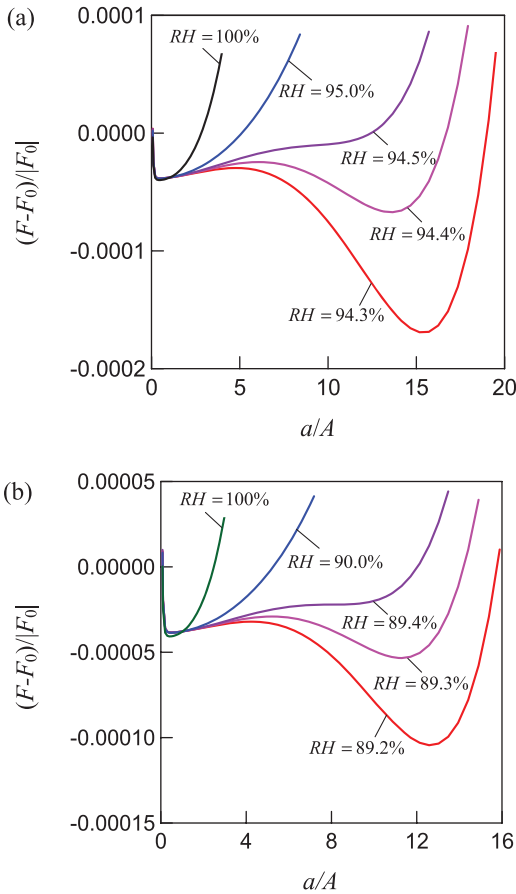


FIG. 2. The free energy landscape of a swollen spherical elastomer containing a cavity and constrained by a rigid shell at different humidity. The initial swelling ratio in (a) is  $\lambda_0 = 1.436$  and in (b) is  $\lambda_0 = 1.307$ . In the calculation, surface energy density is taken as  $\gamma\lambda_0/(NkTA) = 20$ .  $F_0$  is the free energy of the same elastomer without cavity.

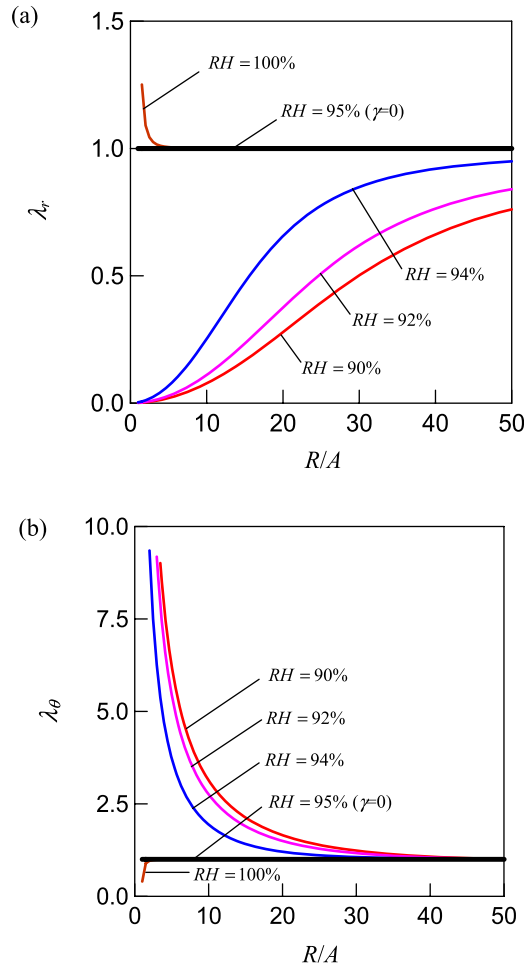


FIG. 4. The distribution of (a) radial stretch and (b) hoop stretch in a swollen elastomer constrained by a rigid shell for different humidity. The initial swelling ratio of the elastomer is  $\lambda_0 = 1.436$ . When the humidity is 95%, with zero surface energy density, there is no deformation in the elastomer as illustrated by the black bold lines in the figure.

at lower humidity for the elastomer with smaller initial swelling ratio.

In Fig. 4, we plot the field of hoop stretch and radial stretch in the elastomer with rigid constraint for different humidity. As shown in Figs. 4(a) and 4(b), for initial swelling ratio  $\lambda_0 = 1.436$ , there is no deformation in the elastomer when the environmental humidity is 95% and surface energy density is assumed to be zero. With nonzero surface energy density ( $\gamma\lambda_0/(NkTA) = 20$ ), when the humidity is higher than 95%, the stretch in radial direction is tensile but in hoop direction is compressive as shown in Figs. 4(a) and 4(b). On the contrary, when the humidity is lower than 95%, we can see compressive stretch in radial direction but tensile stretch in hoop direction. We would like to point out that, in Fig. 4(a), the radial stretch near the cavity surface is very small but always positive. In the calculation, we assume the deformation in the elastomer is elastic. In practice, elastomer may fracture when the deformation is too large.<sup>20</sup>

We next study the effects of the external boundary constraint on the cavitation behavior of the swollen elastomer. Fig. 5 plots the free energy landscape of the core-shell system containing a small cavity. The initial swelling ratio of the swollen core is selected to be  $\lambda_0 = 1.307$ . When the shear modulus of the elastomer shell is large:  $G/(NkT) = 200$  and the surface energy density is  $\gamma\lambda_0/(NkTA) = 20$ , the free energy landscape in Fig. 5(a) is qualitatively similar to

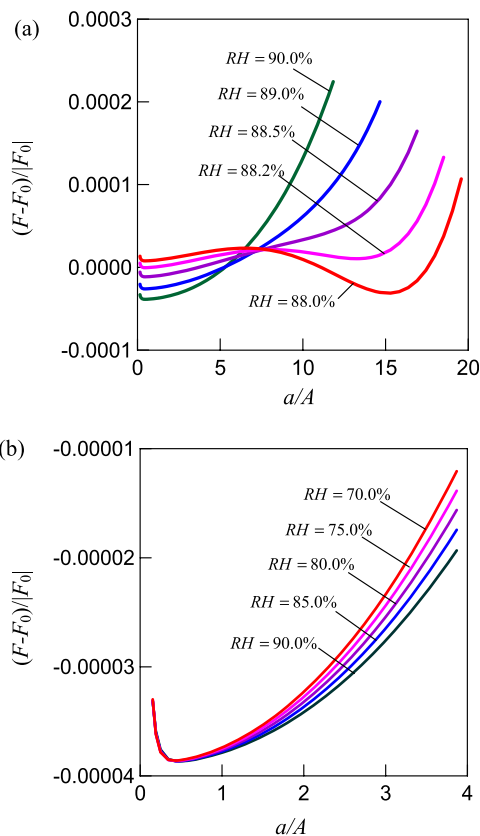


FIG. 5. The free energy landscape of a swollen spherical elastomer containing a cavity and constrained by an elastomer shell at different humidity. The shear modulus of the elastomer shell is (a)  $G/(NkT) = 200.0$  and (b)  $G/(NkT) = 1.0$ . The surface energy density is set to be  $\gamma\lambda_0/(NkTA) = 20$ . The initial swelling ratio is  $\lambda_0 = 1.307$  and  $H/B = 0.256$ .  $F_0$  is the free energy of the same core-shell system without cavity.

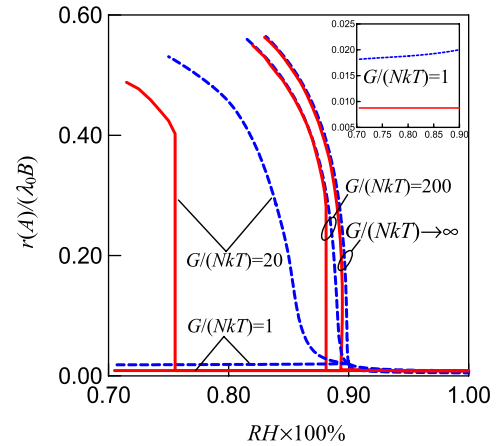


FIG. 6. The size of the cavity in the swollen elastomer constrained by a non-swelling elastomer shell with different shear modulus. The initial swelling ratio of the elastomer is set as  $\lambda_0 = 1.307$ . Solid line is for surface tension  $\gamma\lambda_0/(NkTA) = 20$  and the dashed line is for zero surface tension.

Figs. 2(a) and 2(b), though quantitative difference can be clearly observed. However, when the shear modulus of the shell is reduced to  $G/(NkT) = 1$  with the same surface energy density  $\gamma\lambda_0/(NkTA) = 20$ , only a single well can be found in the free energy landscape (Fig. 5(b)), which indicates that discontinuous change of cavity size in the swollen elastomer will not happen anymore.

Fig. 6 plots the size of the cavity with different constraint as a function of external humidity. The swollen elastomer constrained by a rigid shell has the highest critical humidity for the discontinuous jump of cavity size. With reducing the modulus of the constraint, the critical humidity decreases as well. Discontinuous change of cavity size does not happen when the external elastomer shell is very soft, e.g.,  $G/(NkT) = 1$ . We can also find that for the same environmental humidity, with reducing the elastic modulus of the shell, the cavity size decreases. The size of cavity may even decrease in the drying process due to soft external constraint (the inset of Fig. 6).

#### IV. CONCLUDING REMARKS

We demonstrate the cavitation instability in a core-shell system with swollen elastomer core and non-swelling elastomer shell in the drying process, which may provide some insights into certain failures of swollen elastomers in different environments. We have not noticed any direct or indirect experimental evidence of such cavitation instabilities in swollen elastomers. We plan to conduct experiment to validate our theoretical predictions in the near future.

We would also like to point out that only equilibrium state of the system is calculated in this article. The humidity change is assumed to be much slower than the time for solvent migration. We will investigate the kinetic process of cavitation in swollen elastomers with concerning the solvent migration in our following studies.

#### ACKNOWLEDGMENTS

Huiming Wang acknowledges the support from the National Natural Science Foundation of China (Nos. 11372273

and 11321202) and the Zhejiang Provincial Natural Science Foundation of China (No. LY13A020001). Shengqiang Cai acknowledges the startup funds from the Jacobs School of Engineering at UCSD.

- <sup>1</sup>S. Q. Cai, Y. C. Lou, P. Ganguly, A. Robisson, and Z. G. Suo, *J. Appl. Phys.* **107**, 103535 (2010).
- <sup>2</sup>N. Zalachas, S. Q. Cai, Z. G. Suo, and Y. Lapusta, *Int. J. Solids Struct.* **50**, 920 (2013).
- <sup>3</sup>J. C. Tellis, C. A. Strulson, M. M. Myers, and K. A. Kneas, *Anal. Chem.* **83**, 928 (2011).
- <sup>4</sup>D. Pussak, D. Ponader, S. Mosca, S. V. Ruiz, L. Hartmann, and S. Schmidt, *Angew. Chem., Int. Ed.* **52**, 6084 (2013).
- <sup>5</sup>M. Windisch and T. Junghans, *Adv. Sci. Technol.* **77**, 71 (2013).
- <sup>6</sup>Y. Zhang, H. H. Kim, B. H. Kwon, and J. S. Go, *Sens. Actuators, B* **178**, 47 (2013).
- <sup>7</sup>F. Weiss, S. Q. Cai, Y. H. Hu, M. K. Kang, R. Huang, and Z. G. Suo, *J. Appl. Phys.* **114**, 073507 (2013).
- <sup>8</sup>Z. G. Wu, N. Bouklas, and R. Huang, *Int. J. Solids Struct.* **50**, 578 (2013).
- <sup>9</sup>J. Kim, J. A. Hanna, M. Byun, C. D. Santangelo, and R. C. Hayward, *Science* **335**, 1201 (2012).
- <sup>10</sup>R. Stringfellow and R. Abeyaratne, *Mater. Sci. Eng., A* **112**, 127 (1989).
- <sup>11</sup>W. J. Chang and J. Pan, *J. Mater. Sci.* **36**, 1901 (2001).
- <sup>12</sup>A. Dorfmann and S. L. Burscher, *Plast., Rubber Compos.* **29**, 80 (2000).
- <sup>13</sup>A. N. Gent and C. Wang, *J. Mater. Sci.* **26**, 3392 (1991).
- <sup>14</sup>O. Lopez-Pamies, M. I. Idiart, and T. Nakamura, *J. Mech. Phys. Solids* **59**, 1464 (2011).
- <sup>15</sup>O. Lopez-Pamies, T. Nakamura, and M. I. Idiart, *J. Mech. Phys. Solids* **59**, 1488 (2011).
- <sup>16</sup>S. Wognum, J. M. Huyghe, and F. P. T. Baaijens, *Spine* **31**, 1783 (2006).
- <sup>17</sup>H. M. Wang and S. Q. Cai, *Soft Matter* **11**, 1058 (2015).
- <sup>18</sup>P. J. Flory and J. Rehner, *J. Chem. Phys.* **11**, 521 (1943).
- <sup>19</sup>W. Hong, X. H. Zhao, J. X. Zhou, and Z. G. Suo, *J. Mech. Phys. Solids* **56**, 1779 (2008).
- <sup>20</sup>V. Lefèvre, K. Ravi-Chandar, and O. Lopez-Pamies, *Int. J. Fract.* **192**, 1 (2015).